Theoretical Studies on Proton Transfer Reactions of 8-Hydroxyquinoline Monomers and Dimers

ARTICLE *in* CHINESE JOURNAL OF CHEMISTRY · JUNE 2006

Impact Factor: 1.58 · DOI: 10.1002/cjoc.200690138

6 AUTHORS, INCLUDING:

Yu-Zhong Xie
Yanbian University
9 PUBLICATIONS **36** CITATIONS
SEE PROFILE

wu Xue
Yanbian University
32 PUBLICATIONS **235** CITATIONS
SEE PROFILE

Chinese Journal of Chemistry, **2006**, *24*, 724—730

Full Paper

Theoretical Studies on Proton Transfer Reactions of 8-Hydroxyquinoline Monomers and Dimers

ZHAO, Ji-Yang[a](赵继阳) ZHOU, Zi-Yan*[,a,c](周子彦) SU, Zhong-Min[a,b](苏忠民)
XIE, Yu-Zhong[a](谢玉忠) SUN, Guang-Yan[a](孙光延) WU, Xue[a,c](吴学)

[a] *Department of Chemistry, College of Science, Yanbian University, Yanji, Jilin 133002, China*
[b] *Institute of Functional Material Chemistry, Faculty of Chemistry, Northeast Normal University, Changchun, Jilin 130024, China*
[c] *Key Laboratory of Natural Resources of the Changbai Mountain and Functional Molecules, Ministry of Education, Yanbian University, Yanji, Jilin 133002, China*

Density functional theory (DFT) of quantum chemistry method was employed to investigate proton transfer reactions of 8-hydroxyquinoline (8-HQ) monomers and dimers. By studying the potential energy curves of the isomerization, the most possible reaction pathway was found. The total energy of 8-hydroxyquinoline was lower than that of quinolin-8(1*H*)-one, whereas the order was reversed in dimers. The findings explained the contrary experimental phenomena. The minimum reaction barrier of intramolecular proton transfer was 47.3 kJ/mol while that in dimer was only 25.7 kJ/mol. Hence it is obvious that proton transfer reactions of 8-HQ monomer have a considerable rate but it is easier to proceed for 8-HQ dimer than monomers. It implied that the hydrogen bond played an important role in depressing the activation energy of reaction. The mechanism of the tautomerization was discussed on the basis of theoretical results.

Keywords 8-hydroxyquinoline, proton transfer, tautomerization, density functional theory, transition state

Introduction

Chelate metal complex of 8-HQ is one of the most important electroluminescence materials that have been widely studied from both experimental and theoretical viewpoints.[1-3] In our previous study, we have investigated electroluminescence mechanism of organometallic complexes AlQ_3, GaQ_3 and BeQ_2 by means of *ab initio* HF and DFT B3LYP methods.[4-6] The results indicated that the emissions of organometallic complexes were originated from the electronic π-π* transitions within ligands. In this paper, we will study the properties of the ligand of 8-HQ.

There are many isomers of 8-HQ and they could be isomerized. Tautomerization by proton transfer is not only important for chemical research but also the fundamental for biological research.[7,8] In biological systems, the transport of protons through membrane proteins stores energy for the synthesis of complex biomolecules. We have investigated the isomerization of pyridazine derivatives using DFT B3LYP method,[9,10] while in the present work, we will study the tautomerization of 8-HQ similarly.

Computational methods

All calculations were carried out with the Gaussian 98 program,[11] the geometries of reactants, products and transition states were optimized completely by means of DFT B3LYP method, and vibrational frequencies were calculated at the same level to check whether the obtained stationary points corresponded to isomers or to first order transition states. To confirm the connection of the transition state with designated intermediates, intrinsic reaction coordinate calculations were also performed. The tendencies from TS to either reactant or product were verified and the results proved that the optimized transition states obtained were reliable. In addition, the single-point energies during the reaction process were rectified by zero-point vibrational energies. During calculation, the default value (10^{-8}) defined by the program was adopted as the convergence precision.

Results and discussion

For comparison with experimental results, DFT was used to optimize the structure of 8-hydroxyquinoline, and 6-311G, 6-311G*, 6-311+G, 6-311+G* and 6-311++G basis sets were employed in the present investigation, with the results shown in Table 1.

From Table 1, it could be concluded that the results obtained via the method B3LYP/6-311+G were close to those observed, and calculations in this work were car-

* E-mail: zhouzy@ybu.edu.cn; Tel.: 0086-0433-2732286
Received September 29, 2005; revised December 9, 2005; accepted February 13, 2006.
Project supported by the National Natural Science Foundation of China (No. 20162005) and the Science and Technology Development Program of Jilin Province of China (No. 20020664).

Table 1 Comparison of the observed and calculated geometric parameters and vibrational frequencies of 8-hydroxyquinoline (the windage of calculation results with experimental values)

	C(7)—C(8)/ nm	C(8)—O(17)/ nm	C(9)—N(1)/ nm	N(1)—C(2)/ nm	∠C(7)-C(8)-C(9)/(°)	∠C(7)-C(8)-O(17)/(°)	∠C(9)-N(1)-C(2)/(°)	O(17)—H(18)/ cm^{-1}	C(8)—O(17)/ cm^{-1}
Exp[a]	0.1372	0.1368	0.1374	0.1331	121.4	118.4	117.5	3418	1276
B3LYP/ 6-311G	0.0006	0.0008	−0.0002	−0.0001	−1.3	3.2	0.9	104	15
B3LYP/ 6-311+G	0.0006	0.001	−0.0001	−0.0001	−1.1	2.8	0.9	112	8
B3LYP/ 6-311G*	0.0006	−0.002	−0.0015	−0.0015	−1.7	3.4	0.5	194	27
B3LYP/ 6-311+G*	0.0005	−0.0017	−0.0015	−0.0014	−1.5	3.0	0.6	199	35
B3LYP/ 6-311++G	0.0006	0.001	−0.0001	−0.0001	−1.1	2.8	0.9	112	8

[a] From references 12, 13.

ried out by means of DFT B3LYP under 6-311+G basis set. In this paper, two possible reaction pathways were designed: intramolecular proton transfer, double proton transfer in dimer.

Intramolecular prototropy

Geometric structures of isomers and transition states of 8-HQ monomers in reaction pathways by intramolecular prototropy are shown in Figure 1, with parts of geometric configuration parameters labeled. Zero-point energy, total energy and imaginary frequency are listed in Table 2. Reaction pathways and potential energy surfaces are shown in Figure 2. Meanwhile, variations of the geometric configuration parameters of M1→M2, M2→M3, M2→M9 and M9→M10 during isomerization process are illustrated in Figure 3(a—d).

Calculation results show that the order of total energies of compounds M1—M10 is M5＞M8＞M10＞M6＞M4＞M7＞M9＞M3＞M1＞M2. The energy of M2 is the lowest, which indicates that M2 is the most stable structure among all monomers. As can be seen in Figure 4 (CM_2), when H(18) is on O(17) the conjugate extent of the compound is very large. The distance N(1)—H(18) of M2 is 0.2153 nm, and it is evident that there exits a weak intramolecular hydrogen bond of N⋯H—O to be inferred possibly from the ground-state properties of 8-HQ such as pK_a values or solubility.[14] The calculated ν_{OH} absorption band is at 3530 cm^{-1}, which is due to hydroxyl group vibrations of system with intramolecular hydrogen bonding.[15] Figure 4 displays structures of electron clouds of M2, M9, M6 and M5. From the distribution of the electron clouds, it could be concluded that the conjugate extent of the compound has a direct relation to its stability. The conjugate extent of M5 is the smallest among all the isomers, and the energy of compound M5 is the highest. Isomers M1—M9 all have planar structures, while as for M10, when H(18) was transferred to C(9), the plane of molecule was bent and the largest dihedral angle C(10)-C(9)-C(8)-O(17) was 156.4°.

Table 2 Zero-point vibration energy E_{zp} (a.u.), total energy E (a.u.) (total energy of M1 to be taken as zero) and imaginary frequency (cm^{-1}) of various isomers and transition states in reaction pathways by intramolecular prototropy

Species	E_{zp}	E	ν	Species	E_{zp}	E	ν
M1	0.139090	0	—	TS1	0.138478	0.00391	−424.1
M2	0.140233	−0.01411	—	TS2	0.136257	0.00972	−1361.0
M3	0.140566	0.00293	—	TS3	0.133434	0.11932	−1748.3
M4	0.138301	0.0557	—	TS4	0.133223	0.12613	−1327.0
M5	0.135586	0.09514	—	TS5	0.132888	0.12379	−1304.4
M6	0.137975	0.06137	—	TS6	0.132463	0.13224	−1289.4
M7	0.139151	0.01853	—	TS7	0.134054	0.10011	−1008.0
M8	0.135211	0.09179	—	TS8	0.133988	0.09962	−970.8
M9	0.139018	0.01836	—	TS9	0.133213	0.10548	−2146.3
M10	0.138087	0.06284	—	TS10	0.134124	0.1179	−900.6
				TS11	0.132893	0.10643	−1558.4
				TS12	0.133301	0.12115	−1731.2

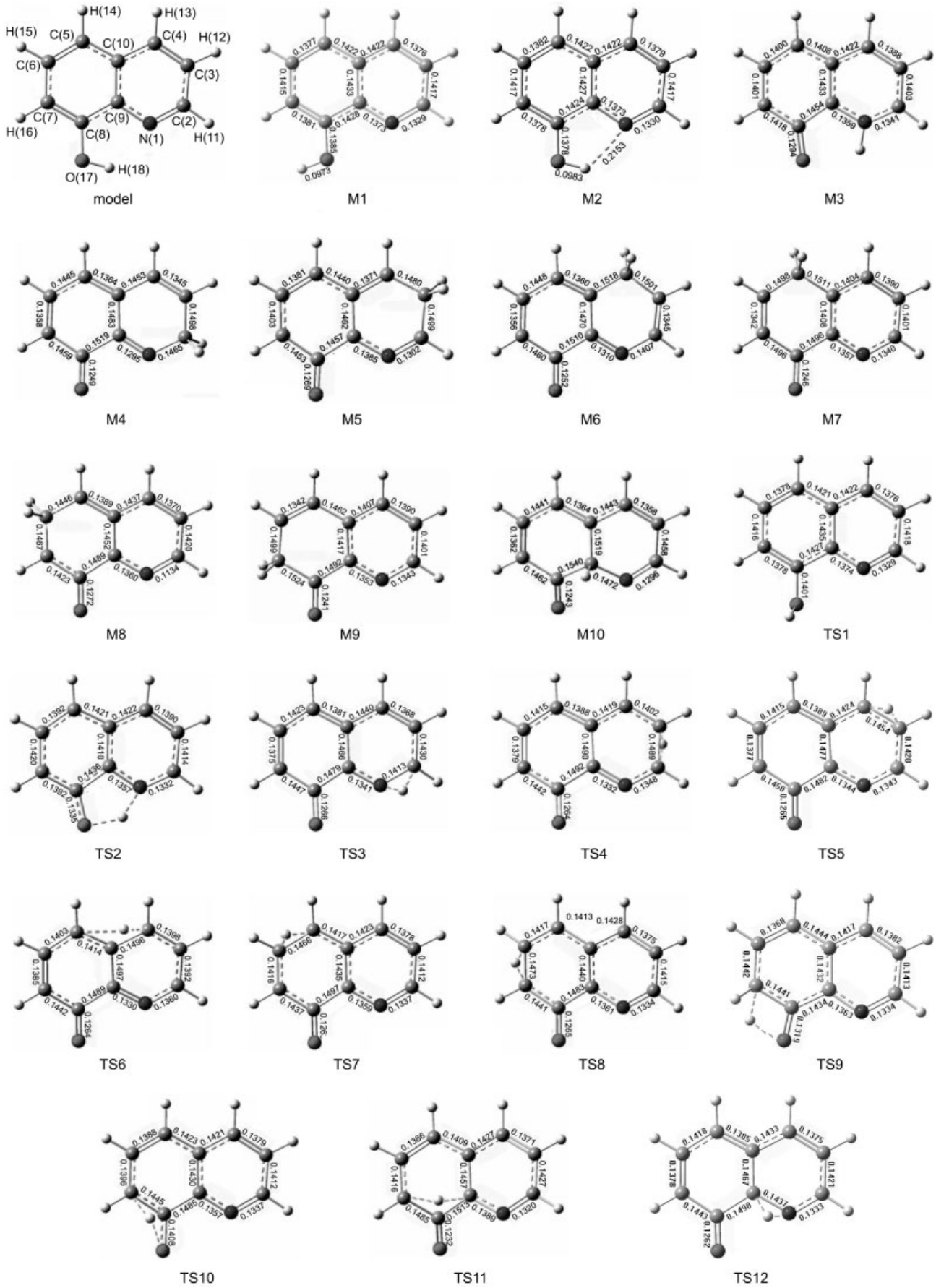

Figure 1 Geometric structures of isomers and transition states of 8-HQ monomers in reaction pathways by intramolecular prototropy (Bond distances are in nm and angles in degree).

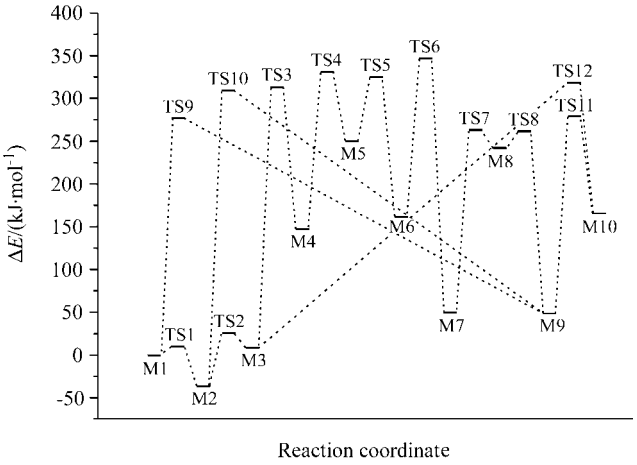

Figure 2 Schematic diagram of potential energy surfaces describing intramolecular proton transfer (kJ/mol, with the energy of M1 taken as zero point).

As shown in Figure 2, M1→TS1→M2 and M2→TS2→M3 are the two reactions that have low barrier to all possible tautomerization reactions. Reaction M1→TS1→M2 is exothermic by 37.1 kJ/mol, and the reaction barrier height is 47.3 kJ/mol, which indicates that the reaction can occur at room temperature. In opposition to the former reaction, M2→TS2→M3 is endothermic by 44.8 kJ/mol with reaction barrier height of 62.6 kJ/mol. As the reverse activation energy is only 17.8 kJ/mol, the reaction may proceed at room temperature with a little probability. The other reactions all have large reaction barrier. For example, the forward reaction activation energy of M3→TS3→M4 is as large as 305.6 kJ/mol. The barrier height is so high that the reaction is very difficult to occur. Consequently among all reaction pathways of intramolecular prototropy, the possible reaction pathways are M1→TS1→M2 and M2→TS2→M3.

In order to ensure the reliability of the calculation results, a bigger basis set of 6-311++G** was used to investigate the prototropy of M1→TS1→M2. Compared to the results calculated with the 6-311+G basis set, geometric structures of the three compounds are nearly the same, and the total energies of them are all lower than the results but the order is the same. In addition, the energy differences with M1 was also similar, and the total energies of them are listed in Table 3.

Table 3 Total energy of M1, TS1 and M2 versus the energy difference with M1 listed in parentheses (a.u.)

	M1	TS1	M2
6-311+G	−476.990930	−476.987016	−477.005044
	(0)	(0.003914)	(−0.014114)
6-311++G**	−477.135489	−477.130454	−477.147297
	(0)	(0.005035)	(−0.011808)

Figure 3(a—d) show the variations of the geometric configuration parameters of M1→M2, M2→M3,

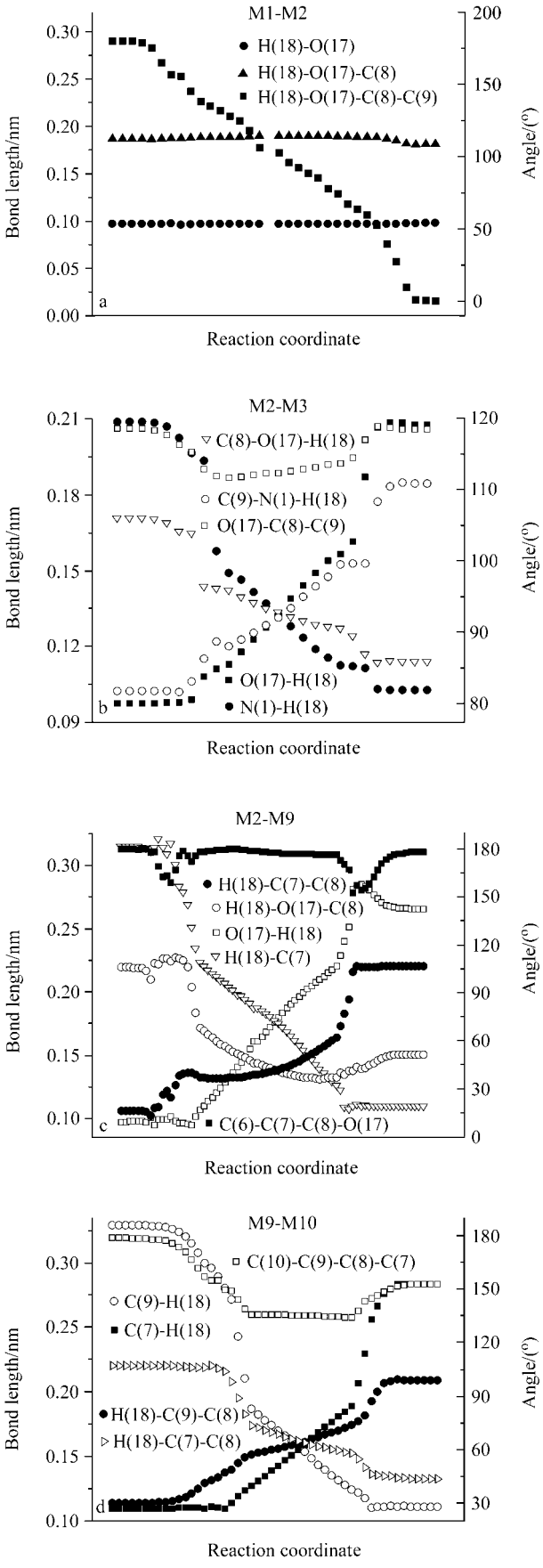

Figure 3 Variations of geometric configuration parameters in the isomerization reaction pathway.

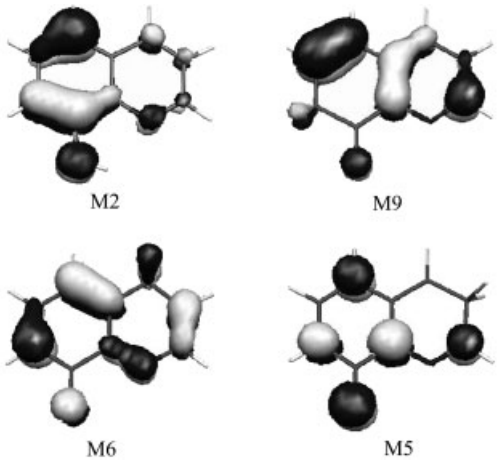

Figure 4 Structures of electron clouds of M2, M9, M6 and M5.

M2→M9 and M9→M10 during isomerization process by analysis of intrinsic reaction coordinate. For example, Figure 3a shows almost no change of bond length of H(18)—O(17) and bond angle of H(18)-O(17)-C(8) during all the reaction process, however only change of dihedral angle of H(18)-O(17)-C(8)-C(9) from about 180° to 0° gradually. Figure 3b shows the variations of the key parts of the geometric configuration parameters of M2→M3 during reaction. As the reaction starts, bond length of O(17)—H(18) is elongated while N(1)—H(18) shrinks gradually. At the same time, bond angle of C(8)-O(17)-H(18) becomes smaller but C(9)-N(1)-H(18) larger. The bond angle of O(17)-C(8)-C(9) is reduced gradually at first, but as the pentanuclear transition state formed it becomes larger slowly. As anticipated by Hammond postulate, the endothermic reaction has a transition state geometry close to the product.[16] When H(18) reaches N(1), the product M3 is formed. Analyses of intrinsic reaction coordinate of other reactions are similar to these.

Double prototropy in dimer

Geometric structures of 8-HQ dimers and their transition state in reaction pathway by intermolecular prototropy are shown in Figure 5, with parts of geometric configuration parameters listed in Table 4. Zero-point energy, total energy and imaginary frequency are shown in Table 5, meanwhile, reaction pathways and potential energy surfaces are shown in Figure 6. Variations of the geometric configuration parameters of M11→M12 during isomerization process are illustrated in Figure 7(a—b).

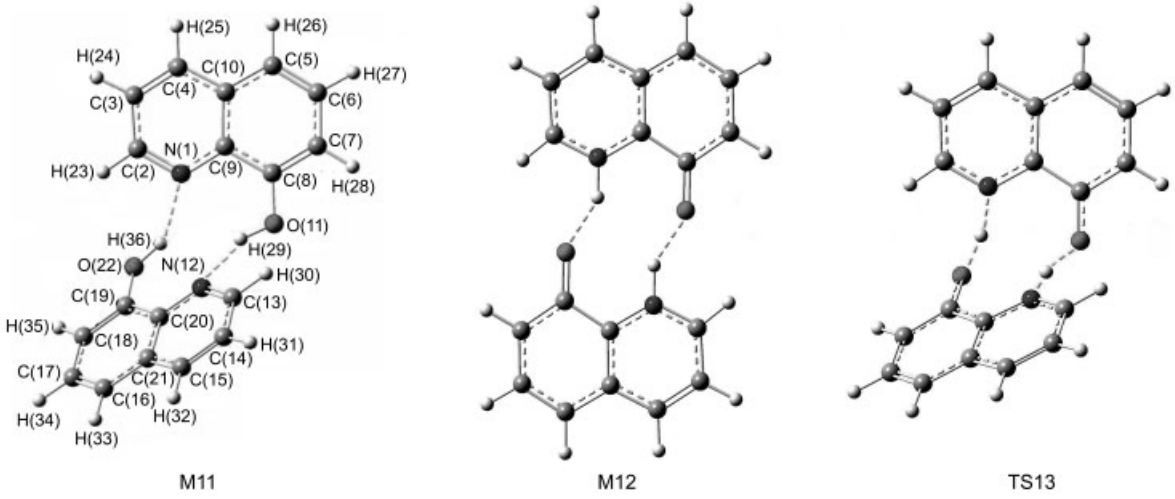

Figure 5 Geometric structures of isomers and transition state of 8-HQ dimers in reaction pathways by intermolecular prototropy.

Table 4 Optimized geometrical parameters of various isomers and transition state in reaction pathway by double-proton transfer of intermolecular in dimer with bond distances in nm and angles in degree

	M11	M12	TS13		M11	M12	TS13
N(1)—C(2)	0.1332	0.1336	0.1333	C(7)-C(8)-O(11)	118.4	123.7	120.2
C(7)—C(8)	0.1386	0.1411	0.1398	C(9)-N(1)-C(2)	119.5	123.7	121.7
C(8)—C(9)	0.1430	0.1448	0.1438	C(8)-O(11)-H(29)	117.9	150.1	127.6
C(9)—N(1)	0.1376	0.1369	0.1374	C(9)-N(1)-H(36)	132.9	121.0	126.2
C(8)—O(11)	0.1365	0.1309	0.1337	C(6)-C(7)-C(8)-C(9)	1.8	0.0	1.8
O(11)—H(29)	0.1013	0.1592	0.1182	C(4)-C(10)-C(9)-C(8)	178.5	−1.0	179.0
N(1)—H(36)	0.1711	0.1058	0.1239	N(1)-O(22)-C(19)-C(18)	145.2	180.0	133.6
C(7)-C(8)-C(9)	119.2	115.3	117.2	N(12)-O(11)-C(8)-C(7)	145.1	180.0	132.6

Table 5 Zero-point vibration energy E_{zp} (a.u.), total energy E (a.u.) and imaginary frequency (cm^{-1}) of various isomers and transition state in reaction pathway by intermolecular prototropy

Species	E_{zp}	E	v
M11	0.280767	−954.3072654	—
M12	0.282282	−954.3097174	—
TS13	0.273245	−954.2999165	−895.8

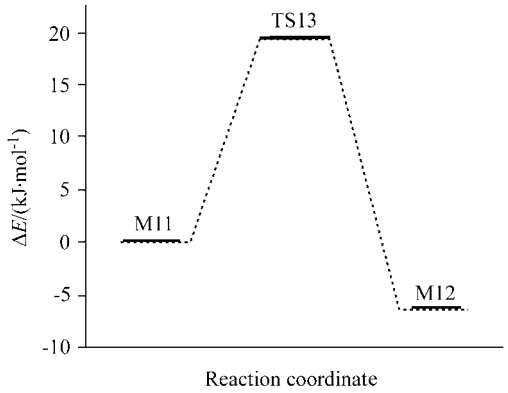

Figure 6 Schematic diagram of potential energy surface describing intermolecular proton transfer (kJ/mol, with the energy of M11 taken as zero point).

As shown in Figure 5, isomer M12 has a planar structure with a long intramolecular [d(H—O)=0.2462 nm] and a short intermolecular [d(H—O)=0.1592 nm] hydrogen bond. However in case of M11 not a planar dimer but the two aromatic planes are twisted by approximately 45.9° against each other. Again a relatively long intramolecular [d(H—N)=0.2548 nm] and a short intermolecular hydrogen bond [d(H—N)=0.1712 nm] were observed. The structure of M11 is similar to the obtained X-ray crystal structure of 8-hydroxy-7-(*S*-1-phenylethylaminocarbamido)quinoline.[17] With respect to 8-HQ monomers, the two 8-HQ dimers are both more stable than compound M2 that is the most stable structure among all monomers. The hydrogen bond has evidently played an important role. In alkane solvents, vapor pressure osmometry measurements in conjunction with infrared spectra show formation of a very stable dimer in the ground state with $K_{dim}=7\times10^7$ at 25 ℃.[18]

The total energy of 8-hydroxyquinoline is lower than that of quinolin-8(1*H*)-one in monomers, whereas the order is reversed in dimers. Either long intramolecular or short intermolecular hydrogen bond of M12 is shorter than that of M11, which suggests the weaker intensity of hydrogen bond of M11 than M12. The difference was used by Baldwin and Langley[19] in the kinetic energy release associated with the mass spectrometric decomposition of metastable molecular ions to investigate the gas phase tautomerism of 8-HQ and 8-hydroxyquinoline was found to exist in the gas phase. However, it was argued by Clugston and MacLean[20] that the quinolinone form was favoured than 8-hydroxyquinoline. The reason

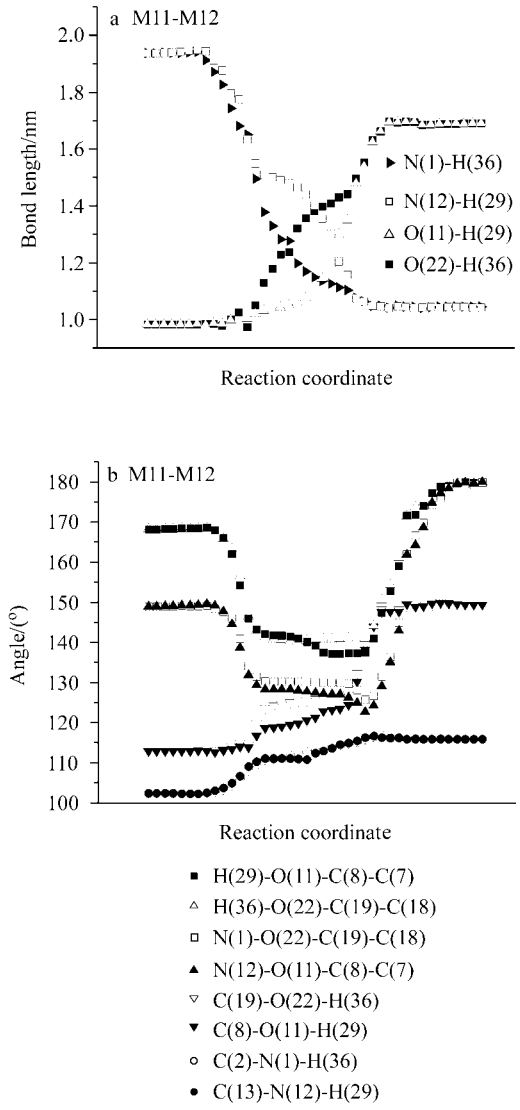

Figure 7 Variations of geometric configuration parameters in the isomerization reaction pathway.

lies in that the 8-HQ was dimerized and there were opportunities for intermolecular processes in Clugston experiment. Whereas by Baldwin and Langley the samples were evaporated directly from the solid phase into a high vacuum in which there was little chance of dimerization and intermolecular reactions. Our calculations are in broad agreement with this and such results are also consistent with Hammond postulate.[16]

As can be seen in Figure 6, reaction of M11→TS13→M12 is exothermic by 6.4 kJ/mol and the reaction barrier height is 25.7 kJ/mol, which is 36.9 kJ/mol lower than the similar proton transfer reaction of M2→TS2→M3. It indicates that tautomerization of 8-HQ dimer is easier to proceed than that of 8-HQ monomer. This is due to the presence of the second molecule that intervenes in the process and relaxes the geometrical structure disposition of the TS. Similar results have been obtained in the tautomeric processes (proton transfer) of an isolated pyrazole molecule when compared to that occurring in the presence of solvent

molecules like water or to the dimer.[21]

As can be seen in Figure 7a and 7b, the distance *d*(H—N) becomes shorter while *d*(H—O) becomes longer with the reaction begins. In the same time, dihedral angle H(29)-O(11)-C(8)-C(7) and N(1)-O(22)-C(19)-C(18) are both reduced gradually, which means that the twist of M11 becomes larger. But after the transition state is formed, the two former dihedral angles become larger and the twist minished. They further react to generate corresponding planar products M12 at last.

Conclusion

Among all monomers, M2 is the most stable for its conjugate extent is very large and there exists a hydrogen bond and because the conjugate extent of M5 is the smallest, M5 is the most unstable. In all possible tautomerization reactions, M1→TS1→M2 and M2→TS2→M3 have low reaction barriers, which are 47.3 and 62.6 kJ/mol, respectively. There are two kinds of hydrogen bond in compounds M11 and M12. M12 is more stable than M11 with the intensity of hydrogen bond of M11 weaker than M12. The stability order in dimers is at variance with that in monomers, which was just in good agreement with experimental results. The reaction barrier height of M11→TS13→M12 is 25.7 kJ/mol, which is 36.9 kJ/mol lower than the similar proton transfer reaction of M2→TS2→M3. It indicates that tautomerization of 8-HQ dimer is easier to proceed than that of 8-HQ monomer.

References

1 Brinkmann, M.; Fite, B.; Pratontep, S.; Chaumont, C. *Chem. Mater*. **2004**, *16*, 4627.

2 Ben Khalifa, M.; Vaufrey, D.; Tardy, J. *Org. Electron*. **2004**, 187.

3 Mirzaee, M.; Amini, M. M. *Appl. Organomet. Chem*. **2005**, *19*, 339.

4 Su, Z. M.; Cheng, H.; Gao, H. Z.; Sun, S. L.; Chu, B.; Wang, R. S.; Wang, Y. *Chem. J. Chin. Univ*. **2000**, *21*, 1416 (in Chinese).

5 Su, Z. M.; Gao, H. Z.; Cheng, H.; Chu, B.; Chen, L. H.; Wang, R. S.; Wang, Y.; Shen, J. C. *Sci. China, Ser. B* **2001**, *31*, 16 (in Chinese).

6 Liao, Y.; Su, Z. M.; Chen, Y. G.; Kan, Y. H.; Duan, H. X.; Qiu, Y. Q.; Wang, R. S. *Chem. J. Chin. Univ*. **2003**, *24*, 477 (in Chinese).

7 Levy, D. H. *Rev. Phys. Chem*. **1988**, *31*, 197.

8 Formosinho, S. J.; Arnaut, L. G. *J. Photochem. Photobiol., A* **1993**, *75*, 21.

9 Zhou, Z. Y.; Pan, X. M.; Wu, X.; Su, Z. M.; Kan, Y. H.; Xie, Y. Z. *Int. J. Quantum Chem*. **2004**, *98*, 515.

10 Zhou, Z. Y.; Wu, X.; Su, Z. M.; Xie, Y. Z.; Pan, X. M.; Ding, W. B. *Acta Chim. Sinica* **2004**, *62*, 2244 (in Chinese).

11 Frisch, M. J.; Trucks, G. W.; Schlegel, H. B.; Scuseria, G. E.; Robb, M. A.; Cheeseman, J. R.; Zakrzewski, V. G.; Montgomery, J. A.; Stratmann, R. E.; Burant, J. C.; Dapprich, S.; Millam, J. M.; Daniels, A. D.; Kudin, K. N.; Strain, M. C.; Farkas, O.; Tomasi, J.; Barone, V.; Cossi, M.; Cammi, R.; Mennucci, B.; Pomelli, C.; Adamo, C.; Clifford, S.; Ochterski, J.; Petersson, G. A.; Ayala, P. Y.; Cui, Q.; Morokuma, K.; Malick, D. K.; Rabuck, A. D.; Raghavachari, K.; Foresman, J. B.; Cioslowski, J.; Ortiz, J. V.; Stefanov, B. B.; Liu, G.; Liashenko, A.; Piskorz, P.; Komaromi, I.; Gomperts, R.; Martin, R. L.; Fox, D. J.; Keith, T.; Al-Laham, M. A.; Peng, C. Y.; Nanayakkara, A.; Gonzalez, C.; Challacombe, M.; Gill, P. M. W.; Johnson, B. G.; Chen, W.; Wong, M. W.; Andres, J. L.; Head-Gordon, M.; Replogleand, E. S.; Pople, J. A. *Gaussian 98*, Revision A3, Gaussian, Inc., Pittsburgh PA, **1998**.

12 Roychowdhury, P.; Das, B. N.; Basak, B. S. *Acta Crystallogr., Sect. B* **1978**, *34*, 1047.

13 Banerjee, T.; Saha, N. N. *Acta Crystallogr., Sect. C* **1986**, *42*, 1408.

14 Bardez, E.; Devol, I.; Larrey, B.; Valeur, B. *J. Phys. Chem. B* **1997**, *101*, 7786.

15 Krishnakumar, V.; Nagalakshmi, R.; Janaki, P. *Spectrochim. Acta, Part A* **2005**, *61*, 1097.

16 Hammond, G. S. *J. Am. Chem. Soc*. **1955**, *77*, 334.

17 Albrecht, M.; Witt, K.; Fröhlich, R.; Kataeva, O. *Tetrahedron* **2002**, *58*, 561.

18 Bardez, E.; Devol, I.; Châtelain, A. *J. Colloid Interface Sci*. **1998**, *205*, 178.

19 Baldwin, M. A.; Langley, G. J. *J. Chem. Soc., Perkin Trans. 2* **1988**, 347.

20 Clugston, D. M.; MacLean, D. B. *Can. J. Chem*. **1966**, *44*, 781.

21 De Paz, J. L. G.; Elguero, J.; Foces-Foces, C.; Llamas-Saiz, A.; Aguilar-Parilla, F.; Klein, O.; Limbach, H. H. *J. Chem. Soc., Perkin Trans. 2* **1997**, 101.

(E0509294 SONG, J. P.; FAN, Y. Y.)